

**NASA Electronic Parts & Packaging (NEPP) Program
Assurance Research on Optoelectronics**

C. Barnes^{*}, M. Ott^{**}, H. Becker^{*}, M. Wright^{*}, A. Johnston^{*}, C. Marshall^{**}, H. Shaw^{**},
P. Marshall^{**}, K. LaBel^{**} and D. Franzen^{*}

^{*}Jet Propulsion Laboratory
California Institute of Technology
Pasadena, CA 91109
(818) 354-4467
charles.e.barnes@jpl.nasa.gov

^{**}NASA Goddard Space Flight Center, Code 735.1
Greenbelt, MD 10771
(301) 286-9936
mott@pop300.gsfc.nasa.gov

ABSTRACT

The wide variety of optoelectronics applications in NASA flight systems and instruments require that optoelectronic technologies meet the demanding requirements of the space environment throughout mission life. These requirements vary widely from intense radiation near Jupiter to the very cold temperatures on the Martian surface to the effects of solar flares in Earth orbit. Considerable work has been performed under the NEPP Program to meet these assurance needs and minimize the risk of insertion of optoelectronics in NASA systems. In this paper we provide recent examples of this work for a variety of NASA mission applications that employ various optoelectronic devices.

1. INTRODUCTION

The qualification of microelectronic and optoelectronic devices for space applications is challenging and difficult because the space environment presents a variety of stressing factors that these devices must survive so that mission success is not jeopardized. As shown in Figure 1 for the various phases of a Mars Lander mission, these environmental factors include a wide variety of effects that can cause optoelectronic devices and circuits to degrade and possibly fail completely. Several of these environmental effects are always present in a NASA mission, such as vibration effects during launch, but the dominant, most severe effect varies dramatically depending on the mission scenario. Unlike missions to the Jovian system where radiation is usually the dominant factor, total ionizing dose (TID) is relatively low for Mars missions such as that in Figure 1, and low temperature effects and contamination, especially for Martian surface assets, can be very important. In contrast, for low Earth orbit (LEO) missions, such as the International Space Station (ISS) and the Shuttle, solar flare-induced radiation effects, both TID and single event effects (SEE), and aging effects for long missions are often significant. The important point to be made, however, is that space qualification of optoelectronics for all NASA missions is difficult and challenging, especially for commercial off-the-shelf

(COTS) optoelectronic components which are not intended for use in the space environment.

The NASA Parts and Packaging (NEPP) Program is a NASA multi-Center Program whose objective is to assess the reliability and radiation tolerance of newly available COTS and emerging electronic and optoelectronic parts and packaging technologies in order to facilitate the low-risk insertion of microelectronics and optoelectronics technologies in NASA systems. In meeting this objective, the NEPP Program evaluates a wide variety of optoelectronics components including optocouplers, LEDs, laser diodes, optical fibers, modulators, detectors, fiber optic links and accompanying conditioning and amplification electronics. These evaluations take into account those environmental parameters that can adversely affect the performance of these optoelectronic components. As indicated in Figure 1, these include operation at very low temperatures, exposure to different types of radiation, damage and misalignment due to mechanical shock and vibration, aging effects and thermal cycling. In this paper, we provide recent examples of this work as an update to our previous review of NEPP work on optoelectronics [1].

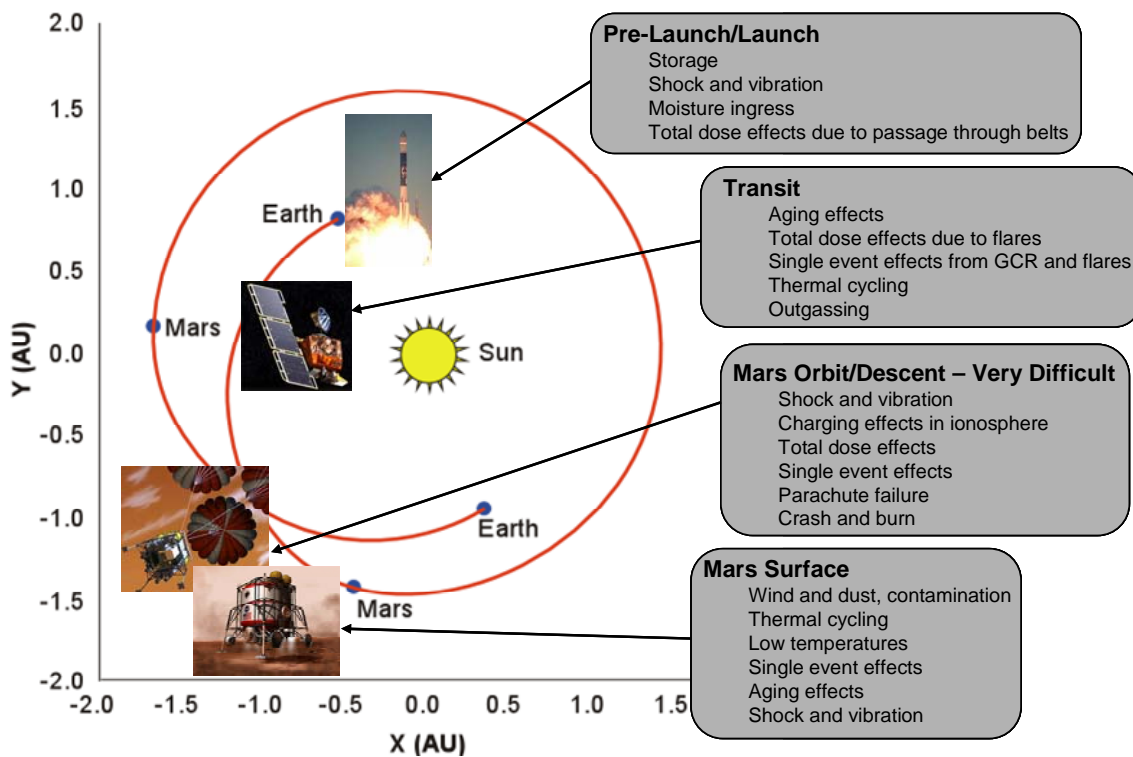


Figure 1. Impact of various space environmental factors on optoelectronic devices for a typical Mars mission scenario [1].

2. LASERS

As indicated in Figure 2, there are a wide variety of NASA applications of lasers, particularly in Earth sensing instruments. These applications require lasers that can withstand the space environment. In this environment, lasers are subject to a wide array of stress mechanisms that can lead to degradation and failure prior to mission completion. Principal among these are radiation effects, aging effects, and laser diode array packaging issues. For example, in the recent GLAS and MOLA missions a variety of packaging failures were observed [2] due to effects including broken solder joints, device shorts due to solder creepage, broken lead wires and intermetallic diffusion. Clearly, the most important stress factor depends on the mission characteristics as noted earlier. In this Section, we provide a few examples of NEPP work on various aspects of laser assurance.

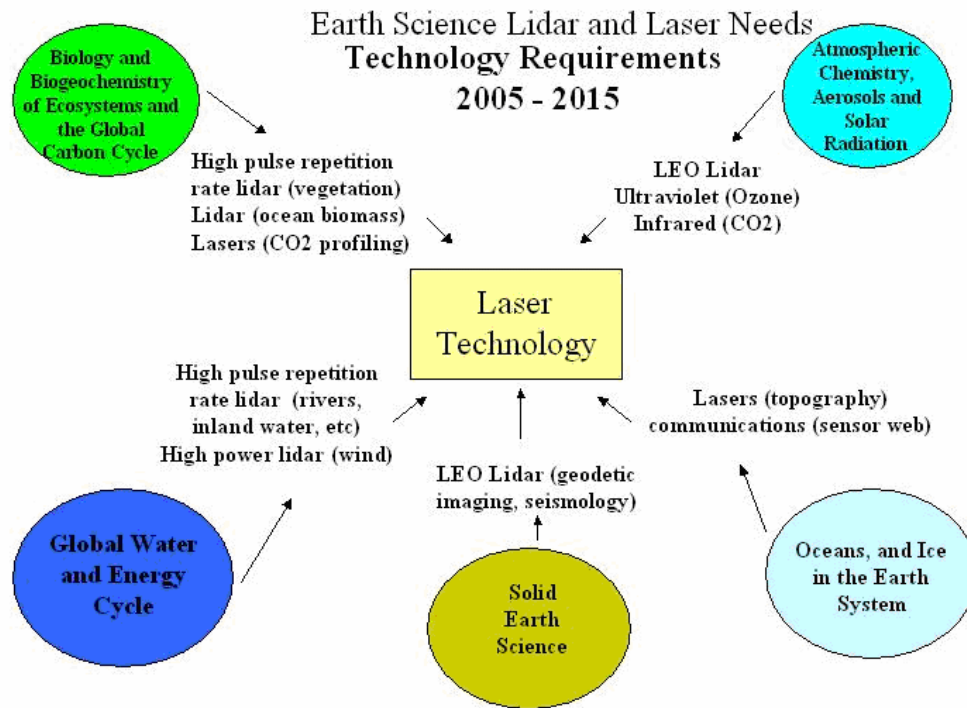


Figure 2: Earth science LIDAR and laser needs in NASA Earth-observing applications.

2.1. Radiation Effects in Injection Laser Diodes (ILDs)

As noted in our earlier review [1], the primary radiation damage mechanism in ILDs for NASA missions is proton-induced displacement damage which causes increases in laser threshold current and reduced power output through the production of non-radiative recombination centers in various regions of the ILD. A variety of state-of-the-art ILDs were examined recently for proton damage effects [3]. These ILDs were fabricated in several material families with an emphasis on InGaAsP devices. A typical ILD structure is shown in Figure 3 which illustrates the multi-layered complexity of these devices.

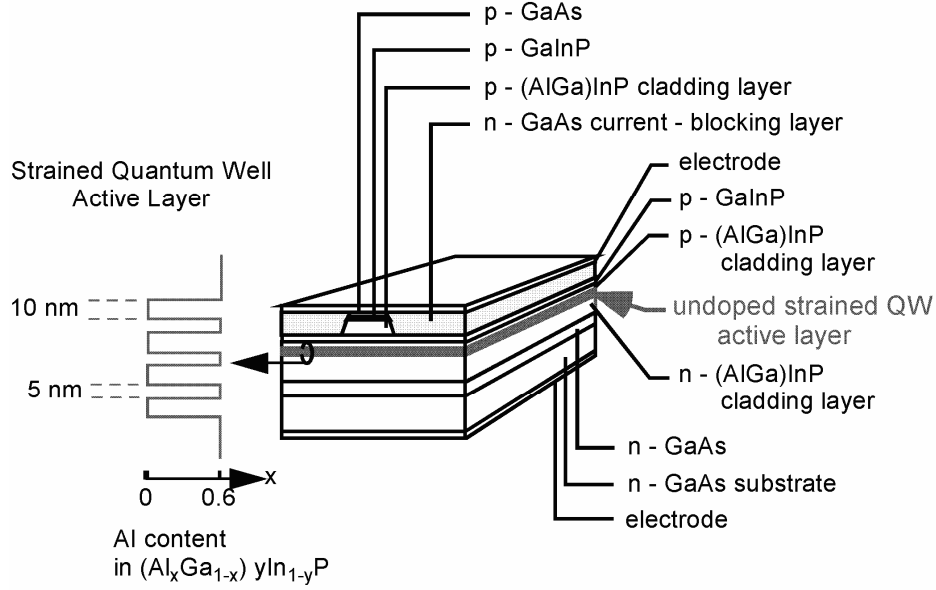


Figure. 3. Diagram of a modern multiple-quantum well in-plane laser diode [3].

The fractional increase in threshold current caused by exposure to 51 MeV protons for a variety of ILDs that emit at different wavelengths is shown in Figure 4 as a function of proton fluence. To first order, the fractional change in threshold current increases linearly with fluence. The two AlGaInP lasers exhibited smaller changes after radiation compared to the other laser types, which may be due to the lower initial operating efficiency of those lasers due to heterostructure leakage.

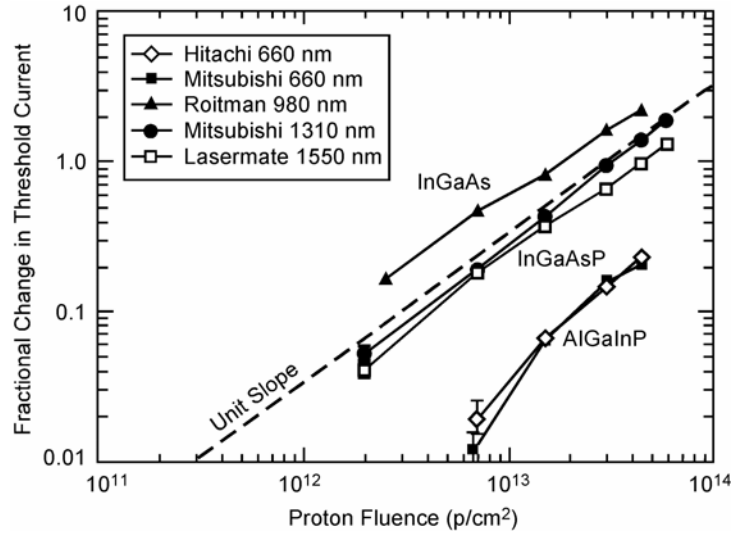


Figure 4. Fractional change in threshold current for the five types of laser diodes, measured at 20°C [3].

In this study [3], the temperature dependence of the threshold current as a function of proton fluence was also examined. Since the temperature range of operation in a

typical NASA application is often wider than that specified for commercial devices, the temperature dependence of the device performance is an important parameter. The larger temperature sensitivity observed for the 1300 and 1550 nm lasers fabricated with InGaAsP is due to the presence of Auger recombination in these ILDs [4]. The temperature dependence of the other three laser types is much lower, and was essentially unaffected by radiation. The temperature dependence of both types of InGaAsP lasers decreased after irradiation, as shown in Figure. 5. The 1300 nm laser was more strongly affected by temperature prior to irradiation and was also more strongly affected by radiation damage. The reduction in threshold current temperature dependence with fluence can be viewed as an offsetting positive influence of radiation exposure because a wide variation in threshold current over the application temperature range is often difficult to accommodate.

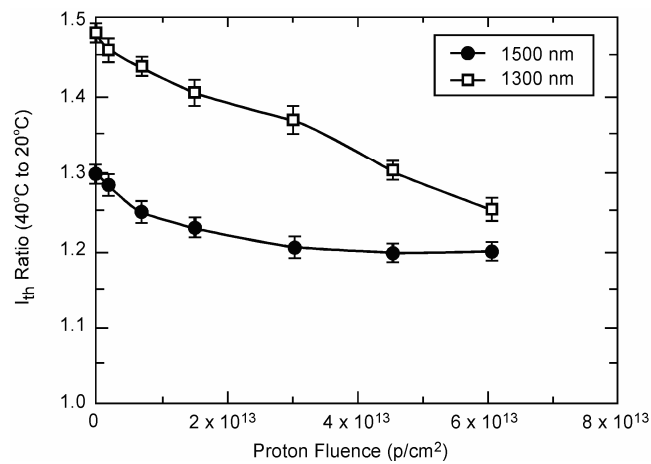


Figure 5. Change in temperature sensitivity of threshold current after irradiation for the two types of laser diodes fabricated with InGaAsP [3].

2.2. Radiation Effects in Vertical Cavity Surface Emitting Lasers (VCSELs)

VCSELs may become the laser source of choice for numerous NASA applications, supplanting both LED and edge-emitting laser sources for data communication, optical interconnections and science instrument applications. There are significant performance, producibility, and packaging advantages exhibited by VCSEL technologies. For example, lower operating currents and power dissipation/emission, high reliability, wafer-level batch fabrication, on-wafer testability, increased fiber coupling efficiency and simplified drive electronics. Additionally, VCSELs are suitable for 1- and 2-dimensional array integration for parallel optical interconnects.

GSFC has performed cobalt 60 and proton irradiation testing on a variety of commercial VCSELs and VCSEL-based data links, and found them to be very robust in each case [5]. The Honeywell HFE-4080 ion implanted 850 nm VCSEL as well as a series of developmental oxide confined Honeywell VCSELs were exposed to multi-MegaRad levels of 63 MeV protons with only small threshold current shifts as well as some reduction in the slopes of the light output versus drive current curves at the higher proton fluences.

These results are consistent with other observations in the literature [6-8]. Similar hardness levels were observed for off-the-shelf gigabit ethernet transceivers that employ 850 nm VCSEL-based transmitters.

2.3. Radiation Effects in Fiber Lasers

Recently, a survey [9] was made under the NEPP Program of the space readiness of doped fiber laser/amplifiers. While many of these laser types are still considered emerging technologies, they will play an important and enabling role in NASA systems. Because fiber lasers contain significant concentrations of dopants, primarily Erbium, they are expected to be sensitive to ionizing radiation. In this study [9], the effect of dopant type on radiation response was examined. Surprisingly, a comparison of different dopant contents shows that the rare earth dopant necessary for laser action is not always the determining factor in radiation induced loss in the fiber. This is demonstrated below in Tables 1 and 2 where Al content dominates radiation response (Table 1) and variations in Er content do not change radiation sensitivity (Table 2). These results suggest that appropriate rare earth dopant levels can be achieved for laser operation without compromising radiation tolerance, an important result for NASA applications.

Table 1: Summary of results comparing two Yb-doped fibers [10].

Rare Earth Optical Fiber	Yb (mol %)	Al ₂ O ₃ (mol %)	P ₂ O ₅ (mol %)	TID	Radiation Induced Attenuation
1*	0.13	1.0	1.2	14 Krads	1 dB/m
2	0.18	4.2	0.9	14 Krads	12 dB/m

*Fiber 1 also contains 5.0 mol% of Germanium

Table 2: Summary of sensitivity results comparing two Er-doped fibers [11].

Rare Earth Doped Optical Fiber	Er Content	Al (%mol wt)	Ge (%mol wt)	Sensitivity 980 nm (dB/m Krad)	Sensitivity 1300 nm (dB/m Krad)	Sensitivity 1550 nm (dB/m Krad)
HE980	$4.5 \cdot 10^{24} \text{ } ^3/\text{m}$	12	20	.013	.0041	.0025
HG980	$1.6 \cdot 10^{25} \text{ } ^3/\text{m}$	10	23	.012	.0038	No data

2.4. Thermal Properties of VCSELs Mounted on Diamond

An important reliability issue for ILDs in general, and VCSELs in particular, is effective heat removal from the laser diode. This is very critical for laser diode bar arrays and for 2-dimensional arrays of VCSELs. For long life NASA missions it is essential to minimize laser degradation due to continuing exposure to high temperatures due to inefficient heat extraction. The importance of this issue led to a study [12] and evaluation of VCSELs mounted on CVD diamond rather than the more typical Kovar mounting headers, which were also included as controls.

Typical results for four VCSELs mounted on diamond headers are shown in Figure 6 for over-driven conditions at 6.25 V. Note that there is essentially no decrease in power output under these conditions. In contrast, at this bias, the Kovar mounted devices failed in a few days. Thus, the VCSELs mounted on diamond were capable of being overdriven at higher current levels without damage compared to the Kovar mounted devices. The highly accelerated voltage and current stress demonstrated that the diamond substrate provided a significant margin of thermal mitigation. VCSELs were driven at up to 3X the manufacturer's recommended maximum instantaneous operating current and 10X the typical threshold current. Thus, one would expect diamond mounted VCSELs to exhibit greater reliability for long life NASA missions under conditions of near-maximum light output usage of the lasers.

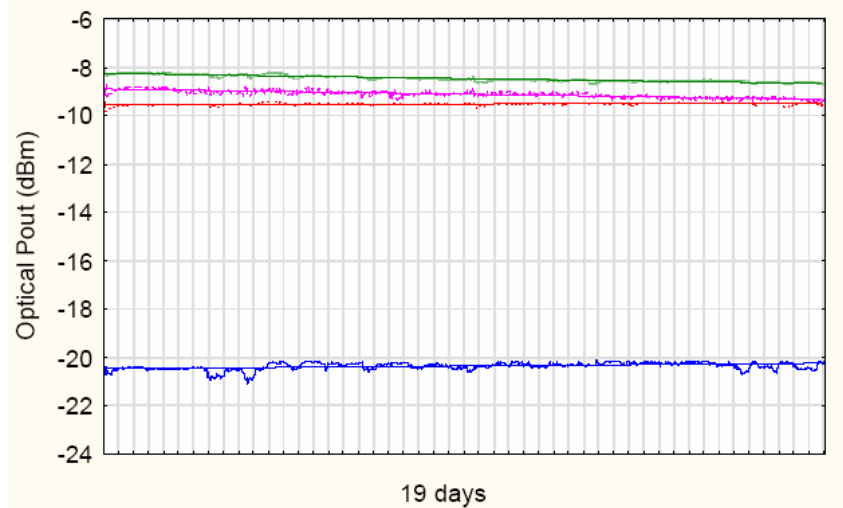


Figure 6. Optical power output characteristics of four VCSELs mounted on diamond headers and operated at 6.25 V at 25°C ambient for 19 days [12].

2.5. Space Qualification of Lasers

Future space missions are increasingly relying on commercial technology for next generation instruments. This means that technology that has not necessarily been designed for the extreme environments of space has to be integrated and tested to ensure the desired performance is sustained within the strict environmental requirements for space borne applications. So-called up-screened commercial-off-the-shelf (COTS) parts are attractive due to the maturity of commercial technologies and the low cost of the parts. A recent study [13] addressed the selection and qualification of a low cost commercial fiber-coupled semiconductor diode pump laser used in a scanning laser radar instrument called Laser Mapper (LAMP) to be used as a guidance and control sensor in future NASA missions.

The qualification and testing process for the commercial pump laser was based on a nonstandard piece part screening plan derived from MIL-STD 883, GSFC 311-INST-001 Rev A and Telcordia standards that apply to optoelectronic devices used in the telecommunications industry. This upsampling plan included mechanical, vibration, thermal cycling, and radiation tests as well as a full destructive parts analysis. Accelerated life

tests were also performed on the packaged devices in order to demonstrate the ability to meet an operational lifetime of 5000 hours. Critical performance parameters for the pump laser, the optical power output and the wavelength stability, were monitored before and after each test to assess the degradation of the laser. The various steps in the upscreening process are shown in Table 3.

Table 3. Pump laser qualification and screening test flow [13].

	Qualification Test	Parameter	Comment
Sample	Accelerated life test 500 hours, 2 W output, 40 °C	λ , Power, Beam Quality	This ensures the design is compatible with the desired reliability
Sample	Destructive Parts Analysis - Visual Inspection - Bond Pull Test - Die Shear test - Fiber Pull test - No Tin on leads verification - Fine and Gross leak - RGA, Internal Moisture - ESD susceptibility		If fiber coupled If hermetic
Sample	Radiation Test, proton dosing, 20 krad(Si)	λ , Power, Beam Quality	Cumulative dosing for material selection
100% screening	Serialization		
100% screening	Opto-electrical characterization, 20 °C	λ , Power, Beam Quality	
100% screening	X-ray or C-SAM Scan		Checks chip attach, voids and cracks
100% screening	Opto-Electrical Characterization	λ , Power, Beam Quality	As above
100% screening	Burn-in 100 hours, 2 W, 40 °C	λ , Power, Beam Quality	Accelerated at high temp to eliminate infant mortality
100% screening	Temperature Cycle -40 °C to 60 °C	λ , Power	8 times, 2° C/min, 10 min dwell at T _{min,max} non-op
100% screening	Opto-Electrical Characterization	λ , Power, Beam Quality	As above
Sample	Particle Impact Noise Detection	λ , Power	Mil Std 883 Meth 2020 B
Sample	Vibration 20 g, 20 – 2kHz	λ , Power	Mil Std 883 Meth 2007.2 Telcordia GR-468-CORE
Sample	Temperature Cycle -40 °C to 60 °C	λ , Power	50 times, 2° C/min, 5° C/min, 10 min dwell
Sample	Constant Acceleration	λ , Power	Mil Std 883 Meth 2001.2
Sample	Opto-Electrical Characterization	λ , Power, Beam Quality	As above
Sample	Mechanical Shock	λ , Power	Mil Std 883 Meth 2002

The results of the upsampling process showed that the selected commercial pigtailed lasers, whose detailed description is given in Reference [13], successfully passed a full qualification testing flow that meets the mission requirements for a LEO orbiting platform. Thus, this study demonstrates that it is possible to select commercial laser devices and through an up-screening and suitable qualification testing process, certify a laser package as space qualified with a reasonable degree of confidence for short term (5000 hrs in this case), risk acceptable missions. One exception that was observed was the constant acceleration test at 5000 g which resulted in failure of all test devices. However, this level of acceleration is well in excess of anything to be experienced by an Earth orbiting satellite throughout its entire mission. A few representative results of the various screening tests are given below.

Life tests of both bare laser diodes and packaged devices were done at a constant current of 3 A and a temperature of 40°C. Results for packaged devices are shown in Figure 7. The “glitch” at about 300 hrs is an experimental artifact. Using an activation energy of 0.4 eV, the lack of any change at 500 hrs and 40°C indicates that the devices will satisfy a mission lifetime requirement of 5000 hrs at a nominal base plate temperature of 25°C.

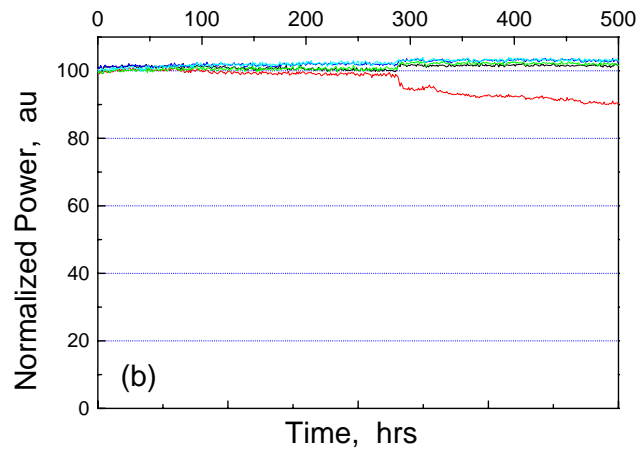


Figure 7. Life-test results from packaged devices at 3A constant current and 40°C [13].

For the thermal cycling upsampling step, devices were cycled at 2°C/min and 5°C/min temperature rates of change over 50 cycles. The dwell times at the temperature extremes of – 30°C and + 50°C were on the order of 10 minutes and the lasers were non-operating during the test. The results, shown in Figure 8, indicate there were no degradation trends. This was even true for a few devices that were heated at 10°C/min for 8 cycles.

The devices were also subjected to the mechanical tests shown in the upsampling flow, and satisfactorily passed the PIND and sinusoidal vibration tests. As noted earlier, the constant acceleration test caused failure, but it was at a much higher g force than expected in the mission. Thus, as pointed out earlier, these packaged laser diodes were qualified for use in an Earth-orbiting, medium life mission.

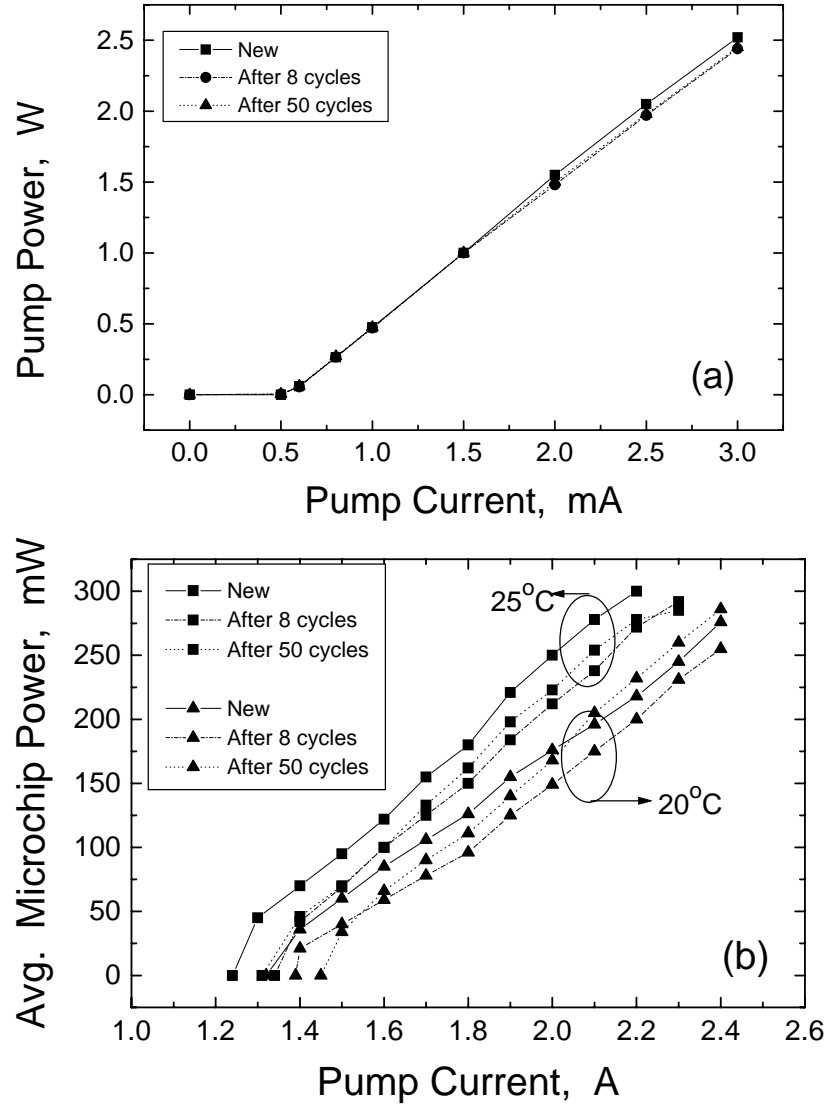


Figure 8. Thermal cycle test results: (a) cw pump diode output power after eight cycles at a 2°C/min and 50 cycles at 5°C/min, and (b) microchip laser average output power for same number of cycles at two different temperature settings [13].

3. Optical Fibers

A variety of studies [14-19] have been conducted recently by Melanie Ott and others at GSFC on optical fibers for space applications. These studies have focused on the problems encountered when one attempts to use commercial optical fiber in a space application. Because of the extreme sensitivity to radiation exhibited by some fibers, these studies are often primarily concerned with a determination of the radiation tolerance of commercial fibers [15,16,18]. Of particular value is the Database Summary [18] of radiation data on commercial optical fiber because it presents comparison tables of radiation data on a large number of fibers, most of which are still available. Such tables allow the designer to select appropriate fibers for particular performance characteristics and

radiation tolerance levels. For example, here we reproduce the table on single mode, polarization maintaining fibers as Table 4 below.

Table 4. Database of radiation effects on polarization maintaining fibers [18].

Fiber ID	λ (nm)	Dose Rate	Total Dose	Temp	Attenuation	Details
PM-M1	850	12 rads/min	17 krad	25 °C	47 dB/km	Actual Experimental Data
	850	12 rads/min	200 krad	25 °C	170 dB/km	Actual Experimental Data
PM-M2	1300	12 rads/min	17 krad	25 °C	1.3 dB/km	Actual Experimental Data
	1300	12 rads/min	200 krad	25 °C	7 dB/km	Actual Experimental Data
PM-M3	1550	10.5 krad/min	500 krad	-55 °C	380 dB/km	Actual Experimental Data
	1550	10.5 krad/min	5 Mrads	-55 °C	480 dB/km	Actual Experimental Data
	1550	10.5 krad/min	10 Mrads	-55 °C	486 dB/km	Actual Experimental Data
	1550	10.5 krad/min	500 krad	25 °C	20 dB/km	Actual Experimental Data
	1550	10.5 krad/min	5 Mrads	25 °C	55 dB/km	Actual Experimental Data
	1550	10.5 krad/min	10 Mrads	25 °C	88 dB/km	Actual Experimental Data
	1550	10.5 krad/min	500 krad	125 °C	15 dB/km	Actual Experimental Data
	1550	10.5 krad/min	5 Mrads	125 °C	92 dB/km	Actual Experimental Data
	1550	10.5 krad/min	10 Mrads	125 °C	135 dB/km	Actual Experimental Data
PM-C1	850	.0083 rads/min	750 rad	25 °C	4.35 dB/km	Actual Experimental Data
	850	.0007 rads/min	10 krad	25 °C	57.8 dB/km	Extrapolated
	850	.0007 rads/min	100 krad	25 °C	578 dB/km	Extrapolated
PM-C2	1300	.0083 rads/min	1.5 krad	25 °C	0.65 dB/km	Actual Experimental Data
	1300	.0007 rads/min	10 krad	25 °C	4.7 dB/km	Extrapolated
	1300	.0007 rads/min	100 krad	25 °C	47 dB/km	Extrapolated
PM-FC1	837	1272 rads/min	10 krad	22 °C	45.6 dB/km	Actual Experimental Data**
PM-FC2	1309	1272 rads/min	10 krad	22 °C	11 dB/km	Actual Experimental Data**

** Data was taken using 10 microwatts of power, where less than 1 microwatt is typical, therefore photobleaching is present.

While for the fiber itself, radiation tolerance is often the primary assurance concern, for fiber cables the reliability of the cable often drives the space qualification of the entire cable. When the connectorization of the fiber cables is included, this further complicates and compounds space qualification issues. This was illustrated by studies of the optical cable fiber assembly for the Mercury Laser Altimeter (MLA) instrument [17,19]. For example, inclusion of connectors in conjunction with fiber cable meant that vibration testing was essential for qualification of the MLA assemblies. Fortunately, as indicated in Figure 9, most of the vibration-induced losses over the 3 minute vibration period were negligible and many were very close to the detector noise floor. There were no vibration-induced losses that registered above 0.004 dB during testing and no final changes in performance greater than 0.003 dB. In several cases the power transmission increased by small amounts (less than .003 dB). A post vibration visual inspection was performed on all mated pairs and the resulting images showed no damage to any of the end faces.

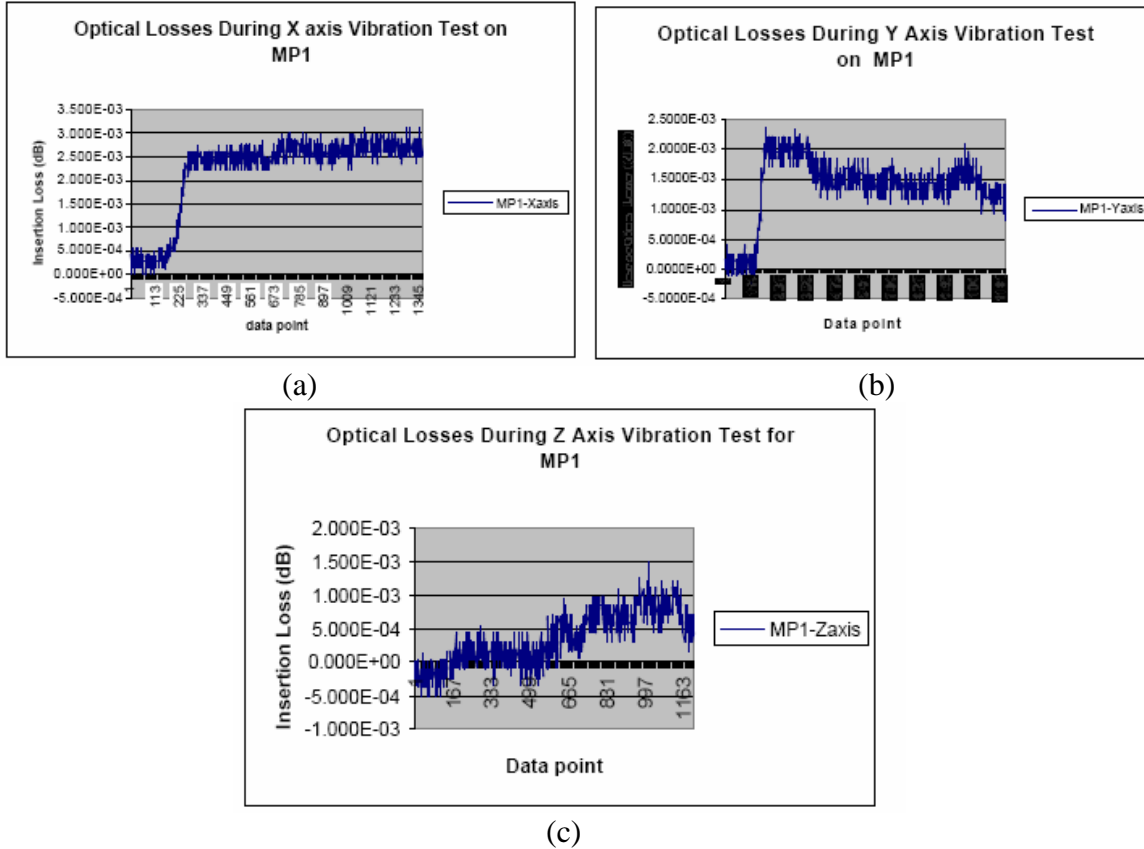
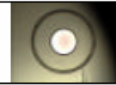
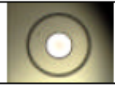






Figure 9. Optical *insitu* monitoring of the relative optical power of MP1 assembly set during 3 minute vibration exposure along the a) X, b) Y axis and c) Z axis [17].

As noted in our earlier review [1], thermal effects can also have significant impact on the reliability of fiber cables. Similar to commercial microelectronics, temperature ranges specified by fiber cable manufacturers for their products are usually significantly narrower than are required for space applications. Additional thermal cycling studies [14,17,19,20] on fiber cables have been performed, and in the case of the connectorized MLA cable, as indicated in Table 5 [17], thermal cycling-induced insertion losses were of the order of a few hundredths of a dB. Thus, the results indicate that the AVIMS assemblies performed quite well with no significant registered insertion losses during or after testing. In all cases the final output power was actually larger than prior to thermal exposure. Comparing the results of the final insertion loss measurements from the vibration testing and the thermal testing it is clear that the effects from thermal testing dominate, but as noted, they are also quite small.

Table 5: Summary of thermal Induced effects on AVIMS assemblies. The largest insertion loss during thermal cycling is listed in column six and the post thermal images of the mated pair that was in the thermal chamber are listed in the last two columns [17].

Assembly	max \leftarrow insertion loss during cycling	Post cycling insertion loss, first 48 cycles	Post cycling insertion loss, additional 42 cycles	Overall Change in insertion loss, 90 cycles.	Max Insertion Loss Registered during Testing	Post Thermal Visual Inspection MPX-1	Post Thermal Visual Inspection MPX-2
MP1	0.09 dB	-0.004 dB*	-0.04 dB	-0.044 dB	0.058 dB	Side A	Side B
MP1							
MP2	0.07 dB	0.015 dB	-0.03 dB	- 0.15 dB	0.037 dB	Side B	Side A
MP2							
MP3	0.04 dB	-0.025 dB	-0.01 dB	-0.035 dB	0.024 dB	Side B	Side A
MP3							

4. DETECTORS

Heidi Becker, et al, have recently published work composed of space readiness reviews of avalanche photodiodes [21,22], and studies of the effects of proton and Co-60 irradiation on avalanche photodiodes [23,24]. As optical communications assumes a greater role in NASA missions, the requirement to thoroughly qualify optical detectors will grow. An important aspect of detector qualification will be the ability to accurately measure the effect of radiation on detector noise characteristics as part of comprehensive radiation testing of advanced optical detectors. The survey [21] and development of test methods lead to a successful characterization of radiation-induced dark current noise spectral density changes in avalanche photodiode structures. The design and construction of the requisite circuitry, and the development of the test methods to perform this type of characterization will be important for NASA's space-based optical communications projects in the future as they qualify optical detectors for radiation environments.

The noise characterization test techniques were employed to examine the effects of proton irradiation and Co-60 irradiation on the noise of three types of Si avalanche photodiodes [24]. An example of the dark current noise response to irradiation of an Advanced Photonix avalanche photodiode is shown in Figure 10. Power line harmonics are evident in initial measurements, but disappear after the noise increases induced by radiation damage due to both 51 MeV protons and Co-60 Gamma rays. Following proton irradiation, dark current noise across the measurement spectrum increased by approximately one decade, and there was a slightly higher increase in the lower frequency (1/f) component of the noise. Although all noise components exhibited annealing, there was less annealing at higher frequencies.

The Co-60 data are noticeably different than the proton data. There was a very high increase in 1/f noise following gamma radiation, and a much smaller increase in high frequency noise. In addition, the post-irradiation DC dark current was almost 50% greater in the sample irradiated with Co-60. Further results and analysis showed that for

both types of radiation, the dominant influence in dark current increases is displacement damage in the depletion layer of the photodiodes, the extent of which is proportional to the volume, and hence the thickness of the depletion layer. It should be pointed out that the Co-60 doses were quite high and enough to introduce significant displacement damage through Compton scattered electron collisions. Thus, for detection of signals with wavelengths near the Si bandgap, which requires deep depletion layers because of the weak absorption, it is more appropriate to use a III-V material-based detector with a smaller, direct bandgap.

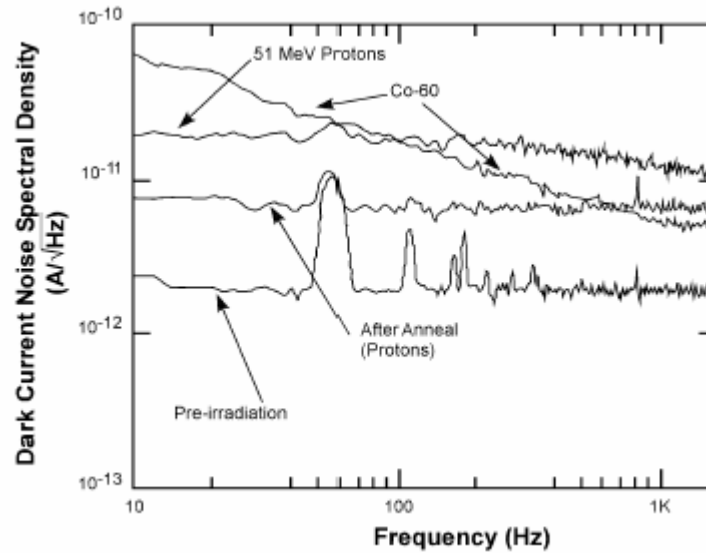


Figure 10. Noise results for the Advanced Photonix (shallow) structure after irradiation to 10^{12} p/cm² or 160 krad(Si) [equivalent total dose] [24].

The need for radiation tolerant detectors operating at wavelengths near and greater than the Si bandgap led to an additional study [23] of avalanche photodiodes fabricated from III-V materials. Their characteristics are shown in Table 6.

The 63 MeV proton-induced increases in dark current in the III-V devices are shown in Figure 11. All three near-infrared APDs showed significant dark current degradation following irradiation with 63-MeV protons. Changes in dark current were linear with fluence for all three device types, but noticeable differences in damage rates were observed. Increases in dark current, compared to pre-irradiation values, ranged from over an order of magnitude in the Ge APD, to four orders of magnitude in the Perkin Elmer InGaAs APD. Changes in dark current increased linearly with fluence at a rate of approximately 4.5×10^{-10} nA-cm²/proton. Very little annealing was observed following irradiation. After one month of unbiased annealing at room temperature, the average reduction in dark current was only 80 nA (approximately 8 %)

Table 6. III-V near infrared avalanche photodiodes examined in radiation study [23].

APD Structure	Active Area Diameter	Cutoff Frequency	QE @ 1300nm	Dark Current (nA)
Hamamatsu <i>InGaAs</i>	30 microns	2 GHz	0.7	~ 6 (M=10)
PerkinElmer <i>InGaAs</i>	80 microns	1 GHz	0.85	~ 1.5 (M=10)
Judson <i>Ge</i>	100 microns	1.5 GHz	0.7	~300 (M=3)

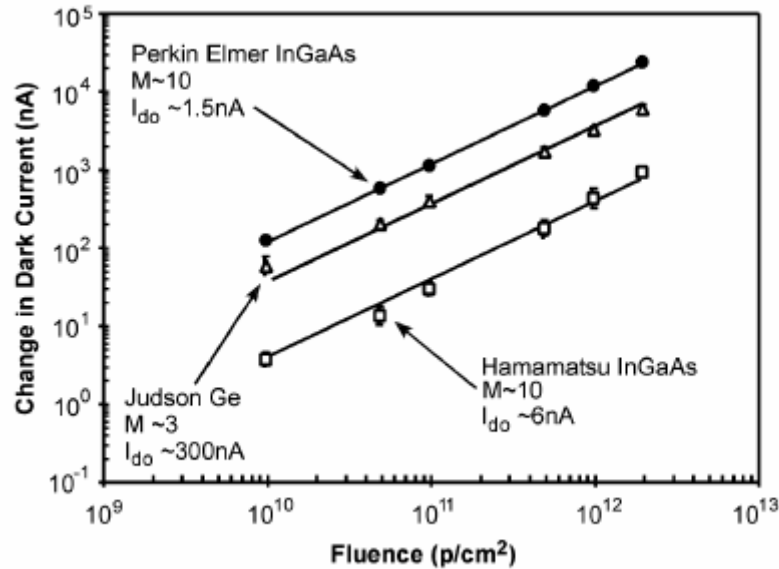


Figure 11. Mean changes in dark current in InGaAs and Ge APDs following exposure to 63-MeV protons [23].

The magnitude of the dark current changes shown in Figure 11 at typical operational gains were similar to the results noted above for silicon APDs, despite the smaller active areas and depletion regions of the APDs examined in the III-V photodiode study [23] (up to four orders of magnitude smaller). This similarity has been attributed to the differences in the material properties of Si, Ge, and InGaAs, and the relative radiation responses of these materials. It was also proposed that the structural complexity of InGaAs APDs makes it difficult to predict their radiation response based on analysis of the volume or doping of the InGaAs absorption region alone.

It should be emphasized that the importance of dark current levels, before or after irradiation, depends entirely on the application and system noise requirements. Wide variations in APD device structure exist. For example, InGaAs APDs use an InP substrate, separate multiplication (InP) and absorption (InGaAs) regions, and an In- GaAsP

transition region to control charge buildup at the heterojunction interfaces. However, there are different InGaAs APD fabrication approaches. Previous work [24] has shown that structural differences can have a large effect on the radiation responses of Si APD technologies, and bulk and surface damage can have varying degrees of dominance depending on structure.

5. CONCLUSIONS CONCERNING OPTOELECTRONICS QUALIFICATION

While we have presented a rather disparate set of examples from recent NEPP Program work on the assurance of optoelectronics for the space environment, one can draw important common factors and important issues from this work and from the broader, community-wide testing and research effort on the use of optoelectronics in space. Important points regarding assurance and qualification include the following (many of these statements are taken from Reference [20] by Melanie Ott):

1. Perhaps the most important conclusion one can draw from the work reviewed herein is that the space qualification of optoelectronic components and subsystems is in many ways still in its infancy. As a result, in spite of the existence of some standards and test protocols, much of the space qualification effort on optoelectronics is unique to a particular mission and does not draw on a body of established test and screening standards and flows. In this sense, optoelectronics in space is at a point equivalent to where Si digital microelectronics was several years ago. It is important to note, however, that significant progress has been made.
2. Unlike Si digital electronics, collectively, the qualification of optoelectronic components represents a wide variety of semiconductor and non-semiconductor materials, and must include materials studies in addition to device qualification efforts, particularly for packaging materials and their materials compatibility.
3. Compared to Si digital and linear microelectronics, the use of optoelectronics in NASA systems is not particularly pervasive as yet. Rather, there are sporadic applications, and this is in part responsible for the relative uniqueness of many qualification procedures, as noted above. As optoelectronics usage in NASA systems becomes more ubiquitous, space qualification methods and protocols will become more universal.
4. Qualification and screening tests for optoelectronics often involve relatively unique and esoteric techniques, the equipment for which is not widespread. This can create problems for flight projects wishing to rapidly and inexpensively qualify optoelectronics.
5. With the exception of high proton fluence space missions (Jupiter and Europa, Mid-Earth orbit), the most common qualification problem for laser diodes and laser diode array modules is the reliability of the packaging and connectorization. For long life missions, these issues can be particularly acute.
6. Of the variety of testing and qualification steps, typified for laser diodes by Table 3, the most important tests are vacuum environment effects, such as

- outgassing onto optical surfaces, vibration effects, radiation effects, temperature performance outside manufacturer specifications and thermal cycling.
7. Because of the wide variety of optoelectronic devices, many of them quite complex, it is important to attempt to discover failure mechanisms in addition to performing a fixed number of screening tests.
 8. When making component selections it is recommended that Telecordia qualified components and vendors be considered first, if there are no military qualified devices available.
 9. Because optoelectronics are rapidly evolving technologies, including the regular appearance of entirely new device types, a flight project cannot usually depend on heritage devices in order to save time and money on qualification.
 10. A balanced and informed approach must be taken with regard to radiation testing and reliability testing. Certain types of tests are expensive and destructive so that, for example, performing expensive radiation tests, such as single event testing, on costly optoelectronic parts that are not reliable should be avoided.
 11. A positive feature of the relatively recent development of many optoelectronic devices is that many suppliers function as custom suppliers and welcome the space business and the participation of project and assurance engineers in the additional development required for space applications.

6. REFERENCES

1. C. Barnes, M. Ott, A. Johnston, K. LaBel, R. Reed, C. Marshall and T. Miyahira, "Recent Photonics Activities Under the NASA Electronic Parts and Packaging (NEPP) Program", *Proc. SPIE Photonics for Space Environments VIII*, **4823**, 189 (2002).
2. H. Leidecker, "Failure analysis of GLAS Laser Diode Arrays", see NEPP Program home page, <http://nepp.nasa.gov/>.
3. A. Johnston and T. Miyahira, "Radiation Degradation Mechanisms in Laser Diodes", *IEEE Trans. Nuc. Sci.*, **51**, 1 (2004).
4. B. Witsigmann and M. S. Hybertsen, "A Theoretical Investigation of the Characteristic Temperature for Semiconductor Lasers", *IEEE J. of Selected Topics in Quantum Electronics*, **9**, no. 3, pp. 807-815, Oct. 2003.
5. M.V. O'Bryan, K.A. LaBel, R.A. Reed, J.W. Howard Jr., R.L. Ladbury, J.L. Barth, S.D. Kniffin, C.M. Seidlick, P.W. Marshall, C.J. Marshall, H.S. Kim, D.K. Hawkins, A.B. Sanders, M.A. Carts, J.D. Forney, D.R. Roth, J.D. Kinnsion, E. Nhan, and K. Sahu, "Radiation Damage and Single Event Effect Results for Candidate Spacecraft Electronics," *2000 IEEE Radiation Effects Data Workshop*, July 2000, pp. 106-122.
6. A.H. Paxton, R.F. Carson, H. Schone, E.W. Taylor, K.D. Choquette, H.Q. Hou, K.L. Lear, and M.E. Warren, "Damage from Proton Irradiation of Vertical-Cavity Surface-Emitting Lasers," *IEEE Trans. Nucl. Sci.*, Vol. 44, No. 6., pp. 1893-1897, 1997.
7. C.E. Barnes, J.R. Schwank, G.M. Swift, M.G. Armendariz, S.M. Guertin, G.L. Hash, and K.D. Choquette, "Proton irradiation effects in oxide-confined vertical cavity surface emitting diodes," presented at the *RADECS99 Conference*, Abbaye de Fontevraud, France, Sept 13-17, 1999, Paper L-O-2.
8. A.H. Johnston, T.F. Miyahira, and B.G. Rax, "Proton Damage in Advanced Laser Diodes," *IEEE Trans. Nucl. Sci.*, Vol. 48, No. 6., pp. 1764-1772, 2001.

9. M. Ott, "Fiber Laser Components Technology Readiness Overview", see NEPP Program home page, <http://nepp.nasa.gov/>.
10. H. Henschel, O. Kohn, H.U. Schmidt, J. Kirchhof, S. Unger, "Radiation-induced loss of Rare Earth doped silica fibers," *IEEE Transactions on Nuclear Science*, Volume: 45 Issue: 3, June 1998, Page(s): 1552 –1557.
11. T. Rose, D. Gunn, G. C. Valley, "Gamma and Proton Radiation Effects in Erbium-Doped Fiber Amplifiers: Active and Passive Measurements," *Jour. of Lightwave Technology*, Volume: 19, Issue: 12, Dec. 2001, Page(s): 1918 –1923.
12. H. Shaw and M. Ott, "Evaluation of Vertical Cavity Surface Emitting Lasers (VCSEL) mounted on CVD Diamond Substrates, see NEPP Program home page, <http://nepp.nasa.gov/>.
13. M Wright, D. Franzen, H. Hemmati, H. Becker and M. Sandor, "Qualification And Reliability Testing Of A Commercial High Power Fiber Coupled Semiconductor Laser For Space Applications", *Optical Eng.*, **44**, 054204 (2005).
14. M. Ott and P. Friedberg, "Technology Validation of Optical Fiber Cables for Space Flight Environments", *Proc. of SPIE: Optical Devices for Fiber Communication II*, **4216**, .206 (2001).
- 15 M. Ott, S. MacMurphy and M. Dodson, "Radiation Testing of Commercial Off-the-Shelf 62.5/125/250 micron optical Fiber for Space Flight Environments", see NEPP Program home page, <http://nepp.nasa.gov/>.
16. M. Ott, "Radiation Hardness of Optical Fiber", see NEPP Program home page, <http://nepp.nasa.gov/>.
17. M. Ott, M. Proctor, M. Dodson, S. MacMurphy and P. Friedberg, "Optical Fiber Cable Assembly Characterization for the Mercury Laser Altimeter", *Proc. of SPIE: Enabling Photonic Technologies for Aerospace Applications V*, **5104**, 96 (2003).
18. M. Ott, "Radiation Effects data on Commercially Available Optical Fiber: Database Summary", see NEPP Program home page, <http://nepp.nasa.gov/>.
20. M. Ott, "Validation of Commercial Fiber Optic Components for Aerospace Environments", *Proc. of SPIE: Smart Structures and Materials 2005: Smart Sensor Technology and Measurement Systems*, **5758**, 427 (2005).
21. H. Becker, "Improved Radiation Qualification & Test Methods: Optical Detector Noise Characterization (Avalanche Photodiodes)", see NEPP Program home page, <http://nepp.nasa.gov/>.
22. H. Becker, "Sensor Technology: Near Infrared Avalanche Photodiodes", see NEPP Program home page, <http://nepp.nasa.gov/>.
23. H. Becker and A. Johnston, "Dark Current Degradation of Near Infrared Avalanche Photodiodes from Proton Irradiation", *IEEE Trans. Nuc. Sci.* **51**, 3572 (2004).
24. H. Becker, T. Miyahira and A. Johnston, "The Influence of Structural Characteristics on the Response of Silicon Avalanche Photodiodes to Proton Irradiation", *IEEE Trans. Nuc. Sci.* **50**, 1974 (2003).

7. ACKNOWLEDGEMENT

The authors wish to thank all those who contributed to the work discussed herein. In addition, we thank NASA OSMA and the NEPP Program Executive, Brian Hughitt for their support of the NEPP Program.